

$K_3B_6O_{10}Cl$: A New Structure Analogous to Perovskite with a Large Second Harmonic Generation Response and Deep UV Absorption Edge

Hongping Wu,^{†,‡} Shilie Pan,^{*,†} Kenneth R. Poeppelmeier,^{*,§} Hongyi Li,[†] Dianzeng Jia,[‡] Zhaohui Chen,[†] Xiaoyun Fan,[†] Yun Yang,[†] James M. Rondinelli,^δ and Haosu Luo^ξ

[†]Xinjiang Key Laboratory of Electronic Information Materials and Devices, Xinjiang Technical Institute of Physics & Chemistry, Chinese Academy of Sciences, 40-1 South Beijing Road, Urumqi 830011, China

[‡]College of Chemistry and Chemical Engineering, Xinjiang University, Urumqi 830046, China

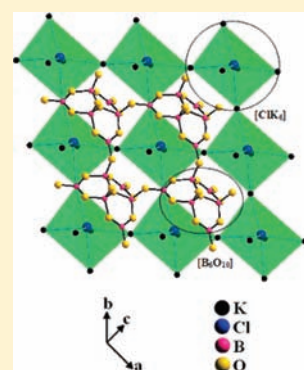
[§]Department of Chemistry, Northwestern University, 2145 Sheridan Road, Evanston Illinois 60208-3113, United States

^δX-Ray Science Division, Argonne National Laboratory, 9700 South Cass Avenue, Argonne Illinois 60439, United States

^ξState Key Laboratory of High Performance Ceramics and Superfine Microstructure, Shanghai Institute of Ceramics, Chinese Academy of Sciences, Shanghai 201800, China

S Supporting Information

ABSTRACT: Introduction of the Cl^- anion in the borate systems generates a new perovskite-like phase, $K_3B_6O_{10}Cl$, which exhibits a large second harmonic response, about four times that of KH_2PO_4 (KDP), and is transparent from the deep UV (180 nm) to middle-IR region. $K_3B_6O_{10}Cl$ crystallizes in the noncentrosymmetric and rhombohedral space group $R3m$. The structure consists of the A-site hexaborate $[B_6O_{10}]$ groups and the BX_3 Cl-centered octahedral $[ClK_6]$ groups linked together through vertices to form the perovskite framework represented by ABX_3 .



INTRODUCTION

Nonlinear optical (NLO) materials^{1–12} have played an important role in laser science and technology, and the search for new NLO materials, particularly for deep-UV and far-IR applications, has attracted considerable attention. One important prerequisite for a material showing NLO properties is that the crystal must be noncentrosymmetric (NCS). Currently, β -BaB₂O₄ (BBO)^{1a} and LiB₃O₅ (LBO)^{1b} are the two most widely used NLO crystals. The $(B_3O_6)^{3-}$ and $(B_3O_7)^{5-}$ groups are considered to be the dominant feature of these NCS structures, respectively. The perovskite structure is also a good candidate for a NCS structure type because it is susceptible to distortions that lead to large second harmonic generation (SHG), for example, in BaTiO₃. It is well-known that the distorted TiO₆ octahedron is the major NLO-active unit in BaTiO₃.^{3c} It is also well-known that the introduction of halogen and alkali metal atoms can widen the transparency of borates in the UV,^{13,14} such as in KBe₂BO₃F₂ (KBBF).^{1c} Thus the incorporation of the alkali cations and halide anions into the borate system may lead to the formation of unique structures. Guided by this idea, we successfully obtained $K_3B_6O_{10}Cl$ (KBOC), which possesses a

perovskite-related structure and has a large SHG response and wide transparency. Herein, we report its synthesis, structure, thermal behavior, UV–vis–IR spectrum, and NLO properties.

EXPERIMENTAL SECTION

Synthesis. Polycrystalline samples of KBOC were prepared via solid-state reaction techniques. Initially, K₂CO₃ (Tianjin Baishi Chemical Reagent Co., Ltd., 99.8%), KCl (Beijing Chemical Co., Ltd., 99.5%), and H₃BO₃ (Beijing Chemical Industry Co., Ltd., 99.5%) were taken in stoichiometric proportions, mixed thoroughly, and preheated in a platinum crucible at 500 °C for 10 h to decompose the carbonate and eliminate the water; the products were cooled to room temperature and ground again. The mixture was then calcined at 720 °C for two days with several intermediate grindings until a single-phase powder was obtained. The powder X-ray diffraction pattern of the bulk polycrystalline phase is in good agreement with the calculated pattern derived from the single-crystal data and is shown in Figure S1 in the Supporting Information.

Received: December 9, 2010

Published: May 02, 2011

Table 1. Crystal Data and Structure Refinement for KBOC

empirical formula	$K_3B_6O_{10}Cl$
formula weight	377.61
crystal system	rhombohedral
space group, Z	$R\bar{3}m$, 3
unit cell dimensions	$a = 10.0624(14) \text{ \AA}$ $b = 10.0624(14) \text{ \AA}$ $c = 8.8361(18) \text{ \AA}$
volume	$774.8(2) \text{ \AA}^3$
density (calculated)	2.428 Mg/m^3
absorption coefficient	$1.623/\text{mm}$
$F(000)$	552
theta range for data collection	3.28° to 27.48°
limiting indices	$-12 \leq h \leq 13$, $-13 \leq k \leq 12$, $-11 \leq l \leq 11$
reflections collected/unique	2606/474 [$R(\text{int}) = 0.0274$]
completeness to theta = 27.48°	100.0%
refinement method	full matrix least-squares on F^2
data/restraints/parameters	474/1/41
goodness-of-fit on F^2	1.188
final R indices [$F_o^2 > 2\sigma(F_o^2)$] ^a	$R_1 = 0.0138$, $wR_2 = 0.0320$
R indices (all data) ^a	$R_1 = 0.0143$, $wR_2 = 0.0323$
absolute structure parameter	$-0.03(4)$
extinction coefficient	$0.066(2)$
largest diff. peak and hole	0.177 and $-0.188 \text{ e} \cdot \text{\AA}^{-3}$

^a $R_1 = \sum ||F_o| - |F_c|| / \sum |F_o|$ and $wR_2 = [\sum w(F_o^2 - F_c^2)^2 / \sum wF_o^4]^{1/2}$ for $F_o^2 > 2\sigma(F_o^2)$ and $w^{-1} = \sigma^2(F_o^2) + (0.0129P)^2 + 0.1902P$ where $P = (F_o^2 + 2F_c^2)/3$.

During the revision of this manuscript, we became aware of a brief structure report of the bromide analogue of KBOC.¹⁵

Crystal Growth. Single crystals of KBOC were grown from a high-temperature solution by using $KF-PbO$ as the flux system. The solution was prepared in a platinum crucible by melting a mixture of KF (Tianjin Guangfu Chemical Reagent Co., Ltd., 99.0%), KCl , PbO (Tianjin Baishi Chemical Reagent Co., Ltd., 99.0%), and H_3BO_3 at a molar ratio of 2:1:2:6. The Pt crucible, which was placed in the center of a vertical programmable temperature furnace, was heated to 650°C at which time the solution became transparent and clear, held at this temperature for 15 h, and then quickly cooled to the initial crystallization temperature. Then, a platinum wire was promptly dipped into the solution. The temperature was further decreased to 490°C at a rate of 0.5°C/h , then the platinum wire was pulled out of the solution and allowed to cool to room temperature. Colorless, transparent crystals had crystallized on the platinum wire. A photograph of one crystal is shown in Figure S2 in the Supporting Information; its crystal dimension is $9 \times 4 \times 2 \text{ mm}^3$, and the obtained average crystal dimension is $4 \times 3 \times 1 \text{ mm}^3$.

X-ray Crystallographic Studies. The crystal structure of KBOC was determined by single-crystal X-ray diffraction on the Rigaku R-axis Spider diffractometer using monochromatic $Mo\ K\alpha$ radiation ($\lambda = 0.71073 \text{ \AA}$) at $293(2) \text{ K}$ and integrated with the SAINT program.¹⁶ A colorless and transparent crystal with dimensions of $0.23 \times 0.20 \times 0.18 \text{ mm}^3$ was chosen for the structure determination. The structure was solved with SHELXS-97¹⁷ by direct methods. All atom positions were refined using full matrix least-squares techniques with anisotropic thermal parameters; final least-squares refinement is on F_o^2 with data having $F_o^2 > 2\sigma(F_o^2)$. The final difference Fourier synthesis map showed the maximum and minimum peaks at 0.177 and $-0.188 \text{ e} \cdot \text{\AA}^{-3}$, respectively. The structure was checked with PLATON.¹⁸ Crystal data and structure refinement information are given in Table 1. The final

refined atomic positions and isotropic thermal parameters are summarized in Table S1 in the Supporting Information. Selected bond distances (\AA) and angles ($^\circ$) are listed in Table S2 in the Supporting Information.

Infrared Spectroscopy. An infrared spectrum was recorded on Shimadzu IRAffinity-1 Fourier transform infrared spectrometer in the $400-4000 \text{ cm}^{-1}$ range. The sample was mixed thoroughly with dried KBr (6 mg of the sample, 500 mg of KBr).

TG/DSC Analysis. The melting behavior of KBOC was carried out on NETZSCH STA 449C simultaneous analyzer instrument. The sample and reference (Al_2O_3) were enclosed in Pt crucibles, heated from 25 to 1000°C at a heating rate of $10^\circ\text{C} \cdot \text{min}^{-1}$ under flowing nitrogen gas.

UV-Vis-IR Transmittance Spectroscopy. The UV-vis-IR transmittance spectrum of the KBOC crystal was collected from 165 to 2600 nm in an atmosphere of flowing N_2 using a Shimadzu SolidSpec-3700DUV spectrophotometer. The plate sample used was 2.08 mm thick and polished on both sides.

Second-Order NLO Measurements. The NCS structure of KBOC prompted us to measure its SHG properties. The test was performed on the microcrystalline samples of the KBOC by the Kurtz-Perry method.¹⁹ Because the SHG efficiency has been shown to depend on particle size,²⁰ polycrystalline KBOC was ground and sieved into distinct particle size ranges, <20 , $20-38$, $38-55$, $55-88$, $88-105$, $105-150$, and $150-200 \mu\text{m}$. Fundamental 1064 nm light was generated with a Q-switched Nd:YAG solid-state laser. The intensity of the frequency-doubled output emitted from the sample was measured using a photomultiplier tube. Microcrystalline KDP served as the standard and was sieved into the same particle size ranges.

Density Functional Calculations. We performed density functional calculations using the Vienna *ab initio* Simulation package (VASP)²¹ within the local density approximation (LDA)²² on the experimentally refined structure. The core and valence electrons were treated with the projector augmented wave method²³ with the following valence configurations: $3s^2 3p^6 4s^1$ (K), $3s^2 3p^5$ (Cl), $2s^2 2p^1$ (B), and $2s^2 2p^4$ (O). The Brillouin-zone (BZ) integrations were performed with a Gaussian smearing of 0.02 eV over a $7 \times 7 \times 7$ Monkhorst-Pack²⁴ k -point mesh centered at Γ and a 550 eV plane-wave energy cutoff. The electronic contribution to the polarization is calculated following the standard Berry-phase formalism.²⁵

RESULTS AND DISCUSSION

Crystal Structure. KBOC crystallizes in the noncentrosymmetric polar rhombohedral space group $R\bar{3}m$. The structure exhibits an intricate three-dimensional network composed of $[B_6O_{10}]$ units and $[ClK_6]$ octahedra (Figure 1) and can also be described as two networks (a $[B_6O_{10}]_\infty$ and a ReO_3 -type ClK_6 net) that are interweaved. The hexaborate $[B_6O_{10}]$ unit consists of three BO_4 tetrahedra (T) shared by the oxygen vertex and three BO_3 triangles (Δ) attached to the terminal vertices of these tetrahedra, which can be represented as $6[3\Delta + 3T]$ according to the definition given by Burns et al.²⁶ The hexaborate units are joined together through their vertices into a new type of $[B_6O_{10}]_\infty$ framework. The individual $[ClK_6]$ Cl-centered octahedra are linked together through vertices to create a distorted perovskite framework. By analogy with the mineral perovskite $CaTiO_3$, the positions of large calcium cations are occupied by the $[B_6O_{10}]$ groups, the positions of titanium atoms are similar to those of chlorine atoms, and the positions of oxygen atoms are similar to the positions of potassium atoms. Hence, their formulas can be represented as $CaTiO_3$ and $[B_6O_{10}]ClK_3$, respectively (Figure 2).

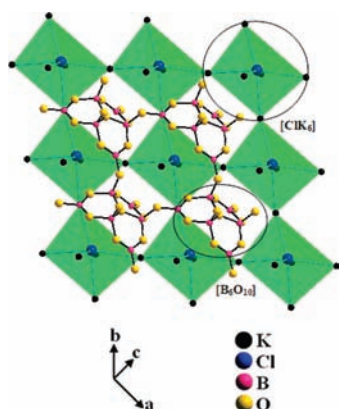


Figure 1. The 3D framework of KBOC with K–O bonds omitted for clarity.

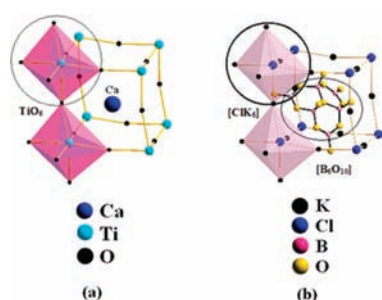


Figure 2. (a) The perovskite structure of CaTiO_3 . (b) The perovskite-related structure of KBOC.

The K cations are bonded to six oxygen atoms and two chlorine atoms (see Figure S3 in the Supporting Information). The K–O bond lengths range from 2.762 to 2.839 Å, an average distance of 2.794 Å. The two K–Cl bond distances lie in a very narrow interval, 3.3101–3.2660 Å. The boron atoms possess two coordination environments, either BO_3 triangles or BO_4 tetrahedra. The B–O distances (1.362–1.373 Å) in BO_3 triangles have an average bond distance of 1.366 Å, which compares with the corresponding B–O bond distances found generally in fluoroborates.^{27,28} O–B–O bond angles are within 2° of the 3-fold symmetrical 120° angle. The BO_4 group exhibits the widest variation of B–O distances (1.448–1.525 Å) and an average bond distance of 1.474 Å, and O–B–O bond angles ranging from 107.02° to 110.94°. These values are in agreement with other borate compounds reported previously.²⁹

Infrared Spectrum. As indicated in Figure S4 in the Supporting Information, the peaks at 1316 and 1176 cm^{-1} can be attributed to asymmetric stretching and symmetric stretching vibrations of BO_3 groups, respectively. The 1006, 877, and 825 cm^{-1} bands are likely the asymmetric and symmetric stretching of B–O in BO_4 , respectively. The deformation vibration at 686, 634, and 597 cm^{-1} can be assigned as the bending of BO_3 groups and 491 cm^{-1} to the bending mode of BO_4 groups.³⁰

TG/DSC Analysis. As shown in Figure S5 in the Supporting Information, there is one endothermic peak on the DSC curve, along with weight loss on the TGA curve upon melting suggesting that KBOC melts incongruently.

UV–Vis–IR Transmittance Spectroscopy. The transmittance spectrum of KBOC from 165 to 2600 nm is shown in Figure 3. Clearly, from 265 to 2400 nm, the transmittance rate is

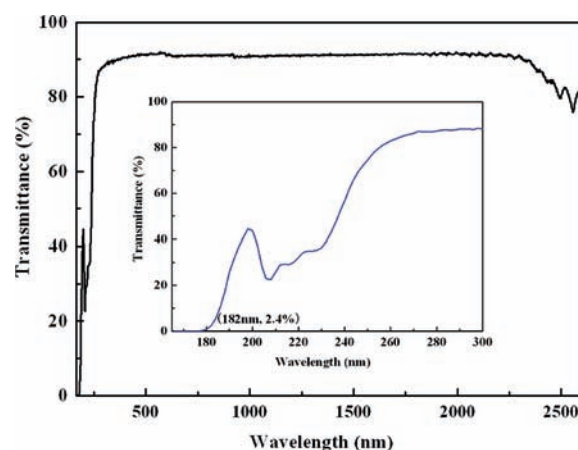


Figure 3. UV–vis–IR transmittance spectrum of KBOC crystal. Inset gives the transmittance versus λ curve between 165 and 300 nm.

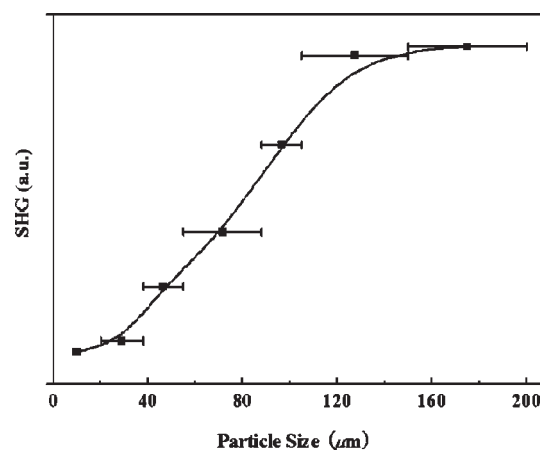


Figure 4. Phase-matching, that is, particle size vs SHG intensity, data for KBOC. The solid curve drawn is to guide the eye and is not a fit to the data.

above 85%, and the transmission rate sharply decreases below 265 nm. There is a peak at 206 nm, which may be from an impurity.³¹ The X-ray diffraction analysis of ground KBOC crystal powder indicates that the impurity may come from KCl. The UV cutoff edge is about 180 nm. Hence KBOC can be used in the deep UV region as a NLO material.

Nonlinear Optical Properties. SHG measurements on the powder samples indicate that KBOC exhibits an SHG efficiency of about 4 times that of KDP, and is phase-matchable as shown in Figure 4. Based on the structural analysis, the polar structural component along the c axis is most pronounced in the boron–oxygen framework (Figure 5). Moreover, it should be noted that the upper and lower triangular faces of the octahedra in the Cl-centered octahedral framework (Figure 6) are asymmetric along the c axis with significantly different K–Cl bond lengths at 3.310 and 3.266 Å ($\Delta l \approx 0.04$ –0.05 Å). Thus, the large response of KBOC is attributed to the cooperative effects of the BO_3 and BO_4 groups and the large degree of polarization of the distorted ClK_6 octahedra. However, the distortions in the ClK_6 octahedra are not the result of second-order Jahn–Teller effects. Furthermore, our dipole calculations based on the point-charge model for the $[\text{B}_6\text{O}_{10}]$ and ClK_6 groups (Figures S6a and S6b in the

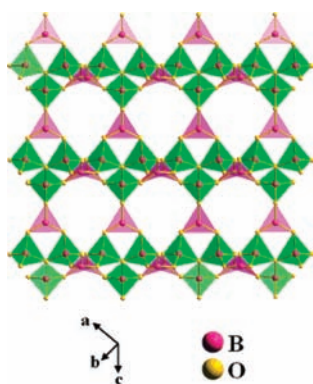


Figure 5. The boron–oxygen framework in the crystal structure of KBOC along the *c* axis; BO_3 triangles and BO_4 tetrahedra are shown in light pink and green, respectively.

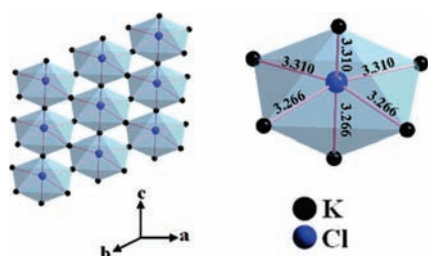


Figure 6. Cl-centered octahedral framework and ClK_6 octahedron.

Supporting Information, respectively) yield 1.635 and 11.330 D, respectively, indicating that distinct acentric distortions exist in both groups. Consistent with these model calculations, our first-principles density functional calculations within the LDA indicate that the total polarization of KBOC is $25.50 \mu\text{C}/\text{cm}^2$ along the *c*-axis. So we conclude that the large SHG response arises from the distortions of $[\text{B}_6\text{O}_{10}]$ groups and ClK_6 groups.

CONCLUSION

The synthesis, structure, and characterization of a new NCS hexaborate, KBOC, are reported. The structure features a three-dimensional network consisting of Cl-centered $[\text{ClK}_6]$ distorted octahedra and hexaborate $[\text{B}_6\text{O}_{10}]$ units. It possesses a UV cut off edge at about 180 nm and is phase-matchable. The perovskite-related structure leads to a large SHG response, about 4 times that of KDP. The density functional calculations within the LDA indicate that the large SHG response comes from not only the $[\text{B}_6\text{O}_{10}]$ groups but also the large degree of polarization of the ClK_6 octahedra. The short UV cut off edge, large SHG response, and wide transparency are favorable for practical applications. Our future research efforts will explore similar systems to find other new NLO materials based on perovskite topologies.

ASSOCIATED CONTENT

S Supporting Information. CIF report, X-ray diffraction pattern data of KBOC compound, the photograph of the KBOC crystal, potassium-coordinated environments, the IR spectrum of KBOC, TGA/DSC curve of KBOC, atomic coordinates and equivalent isotropic displacement parameters, and selected bond

distances and angles. This material is available free of charge via the Internet at <http://pubs.acs.org>.

AUTHOR INFORMATION

Corresponding Author

slpan@ms.xjb.ac.cn; krp@northwestern.edu

ACKNOWLEDGMENT

This work is supported by Main Direction Program of Knowledge Innovation of Chinese Academy of Sciences (Grant No. KJCX2-EW-H03-03), the “National Natural Science Foundation of China” (Grant Nos. 50802110, 21001114), the “One Hundred Talents Project Foundation Program” of Chinese Academy of Sciences, the “Western Light Joint Scholar Foundation” Program of Chinese Academy of Sciences, the “High Technology Research and Development Program” of Xinjiang Uygur Autonomous Region of China (Grant No. 200816120), and Scientific Research Program of Urumqi of China (Grant No. G09212001). K.R.P. acknowledges the National Science Foundation Solid State Chemistry Award No. DMR-1005827. J.M.R. was supported by the U.S. DOE, Office of Science, under Contract No. DE-AC02-06CH11357. Computations were carried out at the Laboratory Computing Resource Center (LCRC) at Argonne National Laboratory.

REFERENCES

- (1) (a) Chen, C. T.; Wu, B. C.; Jiang, A. D.; You, G. M. *Sci. Sin. B* **1985**, *28*, 235. (b) Chen, C. T.; Wu, Y. C.; Jiang, A. D.; You, G. M.; Li, R. K.; Lin, S. J. *J. Opt. Soc. Am. B* **1989**, *6*, 616. (c) Wu, B. C.; Tang, D. Y.; Ye, N.; Chen, C. T. *Opt. Mater.* **1996**, *5*, 105. (d) David, C. *Nature* **2009**, *457*, 953.
- (2) (a) Liao, J. H.; Marking, G. M.; Hsu, K. F.; Matsushita, Y.; Ewbank, M. D.; Borwick, R.; Cunningham, P.; Rosker, M. J.; Kanatzidis, M. G. *J. Am. Chem. Soc.* **2003**, *125*, 9484. (b) Chung, I.; Malliakas, C. D.; Jang, J. I.; Canlas, C. G.; Weliky, D. P.; Kanatzidis, M. G. *J. Am. Chem. Soc.* **2007**, *129*, 14996.
- (3) (a) Muller, E. A.; Cannon, R. J.; Sarjeant, A. N.; Ok, K. M.; Halasyamani, P. S.; Norquist, A. J. *Cryst. Growth Des.* **2005**, *5*, 1913. (b) Halasyamani, P. S.; O’Hare, D. *Chem. Mater.* **1998**, *10*, 646. (c) Halasyamani, P. S. *Chem. Mater.* **2004**, *16*, 3586. (d) Chang, H. Y.; Kim, S. H.; Ok, K. M.; Halasyamani, P. S. *J. Am. Chem. Soc.* **2009**, *131*, 6865.
- (4) (a) Hagerman, M. E.; Poeppelmeier, K. R. *Chem. Mater.* **1995**, *7*, 602. (b) Halasyamani, P. S.; Poeppelmeier, K. R. *Chem. Mater.* **1998**, *10*, 2753. (c) Maggard, P. A.; Stern, C. L.; Poeppelmeier, K. R. *J. Am. Chem. Soc.* **2001**, *123*, 7742. (d) Marvel, M. R.; Lesage, J.; Baek, J.; Halasyamani, P. S.; Stern, C. L.; Poeppelmeier, K. R. *J. Am. Chem. Soc.* **2007**, *129*, 13963.
- (5) (a) Becker, P. *Adv. Mater.* **1998**, *10*, 979. (b) Becker, P.; Bohaty, L.; Froehlich, R. *Acta Crystallogr.* **1995**, *C51*, 1721. (c) Bera, T. K.; Song, J. H.; Freeman, A. J.; Jang, J. I.; Ketterson, J. B.; Kanatzidis, M. G. *Angew. Chem., Int. Ed.* **2008**, *47*, 7828. (d) Paul, A. K.; Sachidananda, K.; Natarajan, S. *Cryst. Growth Des.* **2010**, *10*, 456.
- (6) (a) Wang, S. C.; Ye, N.; Li, W.; Zhao, D. *J. Am. Chem. Soc.* **2010**, *132*, 8779. (b) Zhang, W. L.; Chen, W. D.; Zhang, H.; Geng, L.; Lin, C. S.; He, Z. Z. *J. Am. Chem. Soc.* **2010**, *132*, 1508. (c) Mao, J. G.; Jiang, H. L.; Fang, K. *Inorg. Chem.* **2008**, *47*, 8498. (d) Kong, F.; Huang, S. P.; Sun, Z. M.; Mao, J. G. *J. Am. Chem. Soc.* **2006**, *128*, 7750.
- (7) (a) Chen, C. T.; Liu, G. *Annu. Rev. Mater. Sci.* **1986**, *16*, 203. (b) Ok, K. M.; Halasyamani, P. S. *Chem. Soc. Rev.* **2006**, *35*, 710. (c) Wickleder, M. S. *Chem. Rev.* **2002**, *102*, 2011. (d) Chen, C. T.; Wang, Y. B.; Wu, B. C.; Wu, K. C.; Zeng, W. L.; Yu, L. H. *Nature* **1995**, *373*, 322. (e) Jesudurai, J. G. M.; Prabha, K.; Christy, P. D.; Madhavan, J.; Sagayaraj, P. *Spectrochim. Acta A* **2008**, *71*, 1371.

- (8) (a) Ye, N.; Chen, Q.; Wu, B. C.; Chen, C. T. *J. Appl. Phys.* **1998**, *84*, 555. (b) Hulme, K. F.; Jones, O.; Davies, P. H.; Hobden, M. V. *Appl. Phys. Lett.* **1967**, *10*, 133. (c) Bergman, J. G.; Boyd, G. D.; Ashkin, A.; Kurtz, S. K. *J. Appl. Phys.* **1969**, *40*, 2860.
- (9) (a) Schaffers, K. I.; Deloach, L. D.; Payne, S. A. *IEEE J. Quantum Electron.* **1996**, *32*, 741. (b) Zhang, G. C.; Liu, H. J.; Wang, X. A.; Fan, F. D.; Fu, P. Z. *J. Cryst. Growth* **2006**, *289*, 188.
- (10) (a) Pan, S. L.; Smit, J. P.; Watkins, B.; Marvel, M. R.; Stern, C. L.; Poepplmeier, K. R. *J. Am. Chem. Soc.* **2006**, *128*, 11631. (b) Fan, X. Y.; Pan, S. L.; Hou, X. L.; Liu, G.; Wang, J. D. *Inorg. Chem.* **2009**, *48*, 4806. (c) Li, F.; Hou, X. L.; Pan, S. L.; Wang, X. A. *Chem. Mater.* **2009**, *21*, 2846. (d) Pan, S. L.; Wu, Y. C.; Fu, P. Z.; Zhang, G. C.; Li, Z. H.; Du, C. X.; Chen, C. T. *Chem. Mater.* **2003**, *15*, 2218. (e) Fan, X. Y.; Pan, S. L.; Hou, X. L.; Tian, X. L.; Han, J.; Haag, J.; Poepplmeier, K. R. *Cryst. Growth Des.* **2010**, *10*, 252.
- (11) (a) Rong, C.; Yu, Z.; Wang, Q.; Zheng, S. T.; Pan, C. Y.; Deng, F.; Yang, G. Y. *Inorg. Chem.* **2009**, *48*, 3650. (b) Zhang, C.; Wang, J.; Hu, X.; Jiang, H.; Liu, Y.; Chen, C. *J. Cryst. Growth* **2002**, *235*, 1.
- (12) (a) Hu, Z. G.; Yoshimura, M.; Muramatsu, K.; Mori, Y.; Sasaki, T. *J. Appl. Phys.* **2002**, *41*, 1131. (b) Chen, G. J.; Wu, Y. C.; Fu, P. Z. *J. Cryst. Growth* **2006**, *292*, 449.
- (13) (a) Sasaki, T.; Mori, Y.; Yoshimura, M.; Yap, Y. K.; Kamimura, T. *Mater. Sci. Eng.* **2000**, *30*, 1. (b) Mori, Y.; Yap, Y. K.; Kamimura, T.; Yoshimura, M.; Sasaki, T. *Opt. Mater.* **2002**, *19*, 1.
- (14) Kanai, T.; Kanda, T.; Sekikawa, T.; Watanabe, S.; Togashi, T.; Chen, C. T.; Zhang, C. Q.; Xu, Z. Y.; Wang, J. Y. *J. Opt. Soc. Am. B* **2004**, *21*, 370.
- (15) Al-Ama, A. G.; Belokoneva, E. L.; Stefanovich, S. Yu.; Dimitrova, O. V.; Mochanova, N. N. *Crystallogr. Rep.* **2006**, *51*, 225.
- (16) SAINT, version 7.60A; Bruker Analytical X-ray Instruments, Inc.: Madison, WI, 2008.
- (17) Sheldrick, G. M. *SHELXTL*, version 6.14; Bruker Analytical X-ray Instruments, Inc.: Madison, WI, 2003.
- (18) Spek, A. L. *J. Appl. Crystallogr.* **2003**, *36*, 7.
- (19) Kurtz, S. K.; Perry, T. T. *J. Appl. Phys.* **1968**, *39*, 3798.
- (20) Dougherty, J. P.; Kurtz, S. K. *J. Appl. Crystallogr.* **1976**, *9*, 145.
- (21) (a) Kresse, G.; Furthmuller, J. *Phys. Rev. B* **1996**, *54*, 11169. (b) Kresse, G.; Joubert, D. *Phys. Rev. B* **1999**, *59*, 1758.
- (22) Kohn, W.; Sham, L. J. *Phys. Rev.* **1965**, *140*, A1133.
- (23) Blochl, P. E. *Phys. Rev. B* **1994**, *50*, 17953.
- (24) Monkhorst, H. J.; Pack, J. D. *Phys. Rev. B* **1976**, *13*, 5188.
- (25) King-Smith, R. D.; Vanderbilt, D. *Phys. Rev. B* **1993**, *47*, 1651.
- (26) (a) Grice, J. D.; Burns, P. C.; Hawthorne, F. C. *Can. Mineral.* **1999**, *37*, 731. (b) Burns, P. C.; Grice, J. D.; Hawthorne, F. C. *Can. Mineral.* **1995**, *33*, 1131.
- (27) (a) Alekel, T., III.; Keszler, D. A. *Inorg. Chem.* **1993**, *32*, 101. (b) Lei, S. R.; Huang, Q. Z. *Acta Crystallogr.* **1989**, *C45*, 1861.
- (28) Corbel, G.; Retoux, R.; Leblanc, M. *J. Solid State Chem.* **1998**, *139*, 52.
- (29) (a) Li, F.; Pan, S. L.; Hou, X. L.; Yao, J. *Cryst. Growth Des.* **2009**, *9*, 4091. (b) Wang, Y. J.; Pan, S. L.; Hou, X. L.; Zhou, Z. X.; Liu, G.; Wang, J. D.; Jia, D. Z. *Inorg. Chem.* **2009**, *48*, 7800. (c) Li, Z. H.; Lin, Z. S.; Wu, Y. C.; Fu, P. Z.; Wang, Z. Z.; Chen, C. T. *Chem. Mater.* **2004**, *16*, 2906.
- (30) Li, J.; Xia, S.; Gao, S. *Spectrochim. Acta* **2005**, *433*, 196.
- (31) (a) Liu, L. J.; Liu, C. L.; Wang, X. Y.; Hu, Z. G.; Li, R. K.; Chen, C. T. *Solid State Sci.* **2009**, *11*, 841. (b) Liu, L. J.; Chen, C. T. *J. Cryst. Growth* **2006**, *292*, 472.